# Distributed Channel Access Scheduling for Ad Hoc Networks using Virtual MIMO

Xin Wang †
**wangxin@soe.ucsc.edu**
†Computer Engineering Department,
University of California, Santa Cruz
Santa Cruz, CA 95064, USA

J.J. Garcia-Luna-Aceves †*
**jj@soe.ucsc.edu**
*Palo Alto Research Center (PARC)
3333 Coyote Hill Road
Palo Alto, CA 94304, USA

Hamid R. Sadjadpour ‡
**hamid@soe.ucsc.edu**
‡Electrical Engineering Department,
University of California, Santa Cruz
Santa Cruz, CA 95064, USA

***Abstract*— We propose the distributed CHannel Access scheduling using virtual MIMO Protocol (CHAMP). In CHAMP, nodes build a channel schedule in a distributed fashion to utilize the spatial multiplexing gain of virtual MIMO links. We also use a cooperative relay strategy to fully utilize the available degrees of freedom of virtual antenna arrays. We analyze the single-hop saturation throughput of CHAMP and evaluate its multi-hop performance through simulation. The results show that CHAMP can achieve better performance than a contention-based MAC protocol using MIMO links.**

## I. Introduction

Multiple-input multiple-output (MIMO) techniques can increase the channel capacity significantly through the use of multiple antennas at the wireless transmitter and the receiver. Compared with directional antennas, which suffer significantly without strong line of sight (LOS) components, MIMO is more applicable to fading multipath channels, such as indoor scenarios or other rich scattering environments.

In a point-to-point MIMO channel, the multiple antenna arrays increase the spatial degrees of freedom (DOF) and can provide spatial multiplexing gain or spatial diversity gain [1]. Consider a system with $N$ transmit and $M$ receive antennas, in order to achieve the spatial multiplexing gain, the incoming data are demultiplexed into $N$ distinct streams and each stream is transmitted from a different antenna with equal power at the same frequency. Foschini et al. [2] has shown that the multiplexing gain can provide a linear increase in the asymptotic link capacity as long as both transmit and receive antennas increase. In rich multipath environments, the transmitted data streams fade independently at the receiver and the probability that all data streams experience a poor channel at the same time is reduced. This contributes to the spatial diversity gain of the MIMO channel. In order to achieve spatial diversity gain, each stream is transmitted using different beamforming weights to achieve a threshold gain at the specified receiver while at the same time nulling co-existing, potentially interfering transmitter-receiver pairs. The spatial diversity gain can be used to reduce the bit error rate (BER) or increase the transmission range of the wireless links [3]. We denote by $H_{ij}$ the channel coefficient matrix between sender $i$ and receiver $j$. $H_{ij}$ can be estimated by the receiver through the pilot symbols, but it is unknown at the sender. In order to utilize the spatial diversity gain, the receiver needs to send $H_{ij}$ to the sender.

Spatial multiplexing and spatial diversity gains cannot be maximized at the same time, and so there is a tradeoff between how much of each type of gain any scheme can extract [1]. In this paper, we use virtual antenna arrays to emulate a MIMO system, which can provide some type of antenna gains and have a higher channel capacity. To decide which type of antenna gains should be used in the MAC protocol of ad hoc networks, we compare the design requirements of different antenna gains and analyze their influence on the network capacity. Then we propose a hybrid channel access protocol that allows nodes to establish cooperative transmission scheduling in a distributed fashion.

The rest of the paper is organized as follows. We describe the related work in Section II. We describe the motivation for choosing spatial multiplexing gain and hybrid channel access protocol in Section III. We introduce the details of the proposed approach in Section IV. We numerically analyze the single-hop saturation throughput of CHAMP in Section V. We evaluate the performance of CHAMP under a multi-hop scenario through simulations, and compare it with the alternative design in Section VI. We conclude the paper in Section VII.

## II. Related Work

Sundaresan et al. [4] proposed a fair stream-controlled medium access protocol for ad hoc networks with MIMO links. This work assumes that the receiver can successfully decode all the spatially multiplexed streams when the total number of incoming streams is less than or equal to its DOFs. A graph-coloring algorithm is used to find the receivers that may be overloaded with more streams than they can receive, and then fair link allocation and stream control are applied to leverage the advantage of spatial multiplexing.

SD-MAC [5], NULLHOC [6], and SPACE-MAC [7] all take advantage of spatial diversity. SD-MAC uses the spatial degrees of freedom embedded in the MIMO channels to

[1]This work was supported in part by the Baskin Chair of Computer Engineering at UCSC, the National Science Foundation under Grant CNS-0435522, and the U.S. Army Research Office under grant No.W911NF-041-1-0224. Any opinions, findings, and conclusions are those of the authors and do not necessarily reflect the views of the funding agencies.

improve the link quality and multirate transmissions. It uses the preamble symbols of each packet to convey the channel gains. RTS and CTS are transmitted using a default rate, while data packets are transmitted using multi-rate transmissions. NULLHOC divides the channel into a control channel and a data channel. It uses RTS/CTS handshake in the control channel to keep track of the active transmitters and receivers in the neighborhood and distributes the required transmit and receive beamforming weights. After a receiver obtains an RTS from the transmitter, it calculates its weight vector to null interfering transmissions and conveys the weights to the transmitter using a CTS. The transmitter then calculates its weights to null active receivers in the neighborhood and to obtain unity gain to the desired receiver. Lastly, the receiver and the transmitter convey their selections of weight vectors to all their respective inactive and receiving neighbors. Compared with NULLHOC, SPACE-MAC uses a single channel for the transmision of control and data packets. A node estimates the channel coefficient after it receives the RTS/CTS packets. When a node other than the designated receiver obtains an RTS, it estimates the effective channel matrix and adjusts the weight vector such that the signal from the sender of the RTS is nullified for the duration of time specified in the RTS duration field. When a node other than the sender of the RTS receives the CTS, it estimates the effective channel and stores the weight vector for the duration specified in the CTS duration field.

The Virtual Antenna Array (VAA) approach was first introduced by Dohler [8]. A base-station array consisting of several antenna elements transmits a space-time encoded data stream to the associated mobile terminals which can form several independent VAA groups. Each mobile terminal within a group receives the entire data stream, extracts its own information and concurrently relays further information to the other mobile terminals. It then receives more of its own information from the surrounding mobile terminals and, finally, processes the entire data stream. VAA offers theoretically much more in terms of capacity bounds and data throughput.

Jakllari et al. [9] proposed a multi-layer approach for ad hoc networks using virtual antenna arrays. By using the spatial diversity gain and cooperative transmission among different nodes, their approach forms a virtual MIMO link that increases the transmission range and reduces the route path length. However, this approach requires the virtual MIMO links to be bi-directional. In addition, when there are not enough collaborating nodes around the receiver, the sender cannot cooperate with other nodes to utilize the spatial diversity gain.

## III. Motivation For CHAMP

In this section, we explain why we use the virtual antenna array as our physical layer.

The ergodic (mean) capacity for a complex additive white Gaussian noise (AWGN) MIMO channel can be expressed as [10] [11]:

$$C = E_H\{log_2[det(I_M + \frac{P_T}{\sigma^2 N} HH^\dagger)]\} \quad (1)$$

where $P_T$ is the transmit power constraint, $N$ is the number of transmit antennas, $M$ is the number of receive antennas, $H$ is the channel matrix, $\sigma^2$ is the variance of AWGN and superscript † denotes complex conjugate transpose. $E_H$ denotes the expectation over all channel realizations.

Equation (1) demonstrates that, under the constraint of constant total transmit power per node, increasing the number of receive antennas increases the system capacity. However, with the increase of the transmit antennas, the system capacity becomes a constant if the number of receive antennas is fixed. Based on this observation, we consider the specific virtual MIMO system in this paper shown in Fig 1. Each node can transmit using only one antenna, but can decode simultaneous transmissions using up to $M$ antennas.

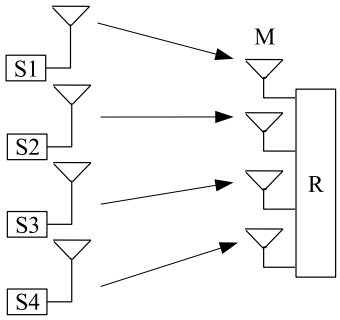


Fig. 1. Virtual MIMO System

The spatial multiplexing gain of the virtual MIMO link cannot be applied directly to an arbitrary MAC protocol. There are several problems in MAC protocol design related to spatial multiplexing gain. First, when the number of simultaneous transmissions is more than the number of receive antennas, the performance of the decoder decreases and the computational complexity of the receiver increases significantly. Hence, to achieve the spatial multiplexing gain, senders need to form a schedule to coordinate the maximum number of simultaneous transmissions. Second, the prerequisite for a virtual MIMO system to increase the throughput of a particular link is for the number of transmitters to be more than the number of receivers. Consider the following example, as Figure 2 shows:

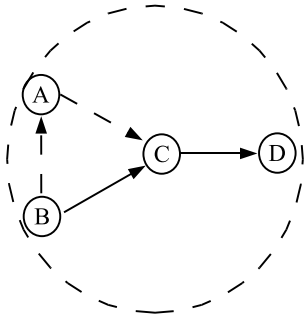


Fig. 2. Cooperative relay example

Using traditional channel scheduling, which lets link $BC$ transmit in slot $i$ and link $CD$ transmit in slot $i+1$, the two-

hop flow $B \rightarrow C \rightarrow D$ cannot utilize the spatial multiplexing gain of virtual MIMO links. We use the cooperative relay transmission among different nodes to address this problem. Now the optimal scheduling consists of first letting $B$ relay packets to $A$ at time slot $i$, and then allowing link $AC$ and $BC$ transmit simultaneously in slot $i+1$, as Table I shows.

TABLE I

COOPERATIVE RELAY EXAMPLE

| Time slot number | $i$ | $i+1$ |
|---|---|---|
| Traditional schedule | $BC$ | $CD$ |
| Optimal schedule | $BA, CD$ | $AC, BC$ |

Based on the above discussion, to fully exploit the spatial multiplexing gain of a virtual MIMO system, the channel scheduling must guarantee that the receiver is not overloaded and that the sender and relay nodes can form the correct cooperation. However, in a multi-hop ad hoc network, it is impossible to use perfect channel scheduling, and randomness has to be used to some extent.

## IV. HYBRID CHANNEL ACCESS USING VIRTUAL MIMO

### A. Assumptions

A time frame can be divided into multiple time slots, as Figure 3 shows. We assume the channel status does not change within a time slot ($T$), which is around $5ms$. A time slot is made up of the contention based access period and the scheduling access period. Each node is synchronized on slot systems and nodes access the channel based on slotted time boundaries. Each time slot is numbered relative to a consensus starting point. The condition that must be true for a receiver to decode all the transmitted data streams is for the number of simultaneous transmissions in the one-hop range to be less than the number of receive antennas.

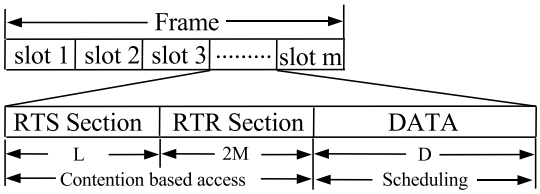


Fig. 3. Time frame and time slot structure

### B. Contention based access period

During the contention-based access period, nodes exchange the neighbor information and form the transmission scheduling. It can be further divided into a request-to-send (RTS) section and a ready-to-receive (RTR) section. Each section is made up of multiple mini-slots. The length of the mini-slot ($T_{\mathrm{m}}$) is:

$$T_{\mathrm{m}} = max(T_{\mathrm{RTS}}, T_{\mathrm{RTR}}) \tag{2}$$

where $T_{\mathrm{RTS}}$ and $T_{\mathrm{RTR}}$ are the transmission time for a RTS/RTR packet, respectively.

*1) RTS Transmission:* The RTS section is used to exchange the neighbor information and the channel-state information. We denote the length of the RTS section as $L$. Each node $i$ generates a random number $n$ which is uniformly distributed between $[1, L]$ and uses mini-slot $n$ to send the RTS packet, which includes the following items:

- The intended receiver $j$ (NULL for broadcast packet, 0 for nodes without any transmissions).
- The past bandwidth share of link $(i, j)$, denoted by $(B_{ij})$ and defined as the percentage of successful transmissions of link $(i, j)$ over the last 50 time slots.
- Pilot symbols (PS) used by the receiver to estimate the channel status and utilize the spatial multiplexing gain.
- The sequence number space of the packets that node $i$ has buffered for each destination.
- The one-hop neighbor list of node $i$ and whether a one-hop neighbor is a *receiver*.

At the end of RTS section, a node that determines that it is the intended receiver of other nodes or hears broadcast transmission request identifies itself as a *receiver*; if a node does not receive an RTS from a neighbor during 10 time slots, it removes the neighbor from the one-hop neighbor list.

*2) Receiver Based Channel Scheduling Formation:* Based on the information collected during the RTS section, each receiver generates a local contention graph $G_c(V_c, E_c)$. The vertex set ($V_c$) of $G_c$ are links in the original topology graph. When two links are in conflict with each other, there is an edge $e \in E_c$ between the corresponding vertexes in $G_c$.

We divide the channel scheduling formation into two steps: original transmission scheduling and relay scheduling.

*a) Original transmission scheduling:* Using original transmission scheduling, a node first decides which original links should be scheduled for transmission in a specific time slot. We denote by $i$ the original transmission link ($i \in V_c$). $B_i$ is the corresponding past bandwidth share indicated in the RTS. We denote the original transmission scheduling by $S_o(t)$, where $t$ is the data slot number of the scheduling based transmission period. $t \in 1, \ldots, D$; and $D$ is the length of scheduling based transmission period, which will be discussed in Section IV-C. The indicator function $I(i, j)$ equals 1 if $(i, j) \in E_c$; otherwise, it equals zero. We formulate the original transmission scheduling problem as follows:

$$\begin{aligned} & max \textstyle\sum_{t=1}^{D} \sum_{i=1}^{|S_o(t)|} logB_i \\ s.t. \quad & I(i,j) = 0, && \forall i,j \in S_o(t), i \neq j \\ & |S_o(t)| \leq M, && \forall t \in 1, \ldots, D \end{aligned} \tag{3}$$

The objective of the optimization is to achieve proportional fairness among different links. The first constraint ensures that the scheduling is collision free. The second constraint guarantees that the number of simultaneous transmissions is smaller than the number of receive antennas.

*b) Relay scheduling:* Given the scheduling for the original transmission links, if the available degree of freedom (DOF) of a receiver in a data slot is more than zero, then we

try to find the relay nodes and utilize cooperative transmissions to increase the spatial multiplexing gain of virtual MIMO links. For each link $(i,j) \in V_c$, there is a relay link set $R_{ij}$ that indicates the links that can be scheduled for transmission simultaneously. $R_{ij}$ is generated as follows:

Let $N_i$ denote the one-hop neighbor set of node $i$ and consider two links $(i,j)$ and $(j,k)$ that coincide with each other in $G_c$. The relay node $r$ is selected as follows:

$$r = N_i \cap N_j \cap \overline{N_k} \tag{4}$$

Then $(i,r) \in R_{ij}$.

After the relay link set $R_{ij}$ is obtained, $S_o(t)$ is modified and the overall throughput is maximized by solving the following optimization problem:

$$\begin{aligned} & max \sum_{t=1}^{D} |S(t)| \\ s.t. \quad & I(i,j) = 0, \qquad \forall i,j \in S(t), i \neq j \\ & |S(t)| \leq M, \qquad \forall t \in 1,\ldots,D \end{aligned} \tag{5}$$

We use the example shown in Figure Figure 4 to illustrate the channel schedule formation process.

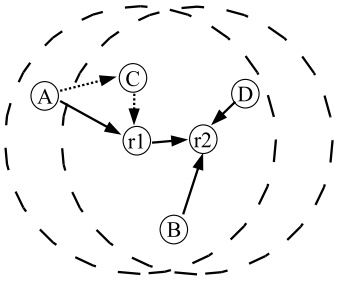


Fig. 4. Channel scheduling formation example

The original transmission links are:

$\{A \rightarrow r1, r1 \rightarrow r2, B \rightarrow r2, D \rightarrow r2\}$

The scheduling results of receiver $r1$ and $r2$ at each step are shown in Table II:

TABLE II

CHANNEL SCHEDULING EXAMPLE

| | slot number | original scheduling | final scheduling |
|---|---|---|---|
| $r1$ | $i$ | $Ar1, Br2, Dr2$ | $AC, r1r2, Br2, Dr2$ |
| | $i+1$ | $r1r2, Br2, Dr2$ | $Cr1, Ar1, Br2, Dr2$ |
| $r2$ | All slots | $r1r2, Br2, Dr2$ | $r1r2, Br2, Dr2$ |

*3) RTR transmission:* The RTR section is used by the receivers to send the RTR that specifies the channel scheduling. We use a fair node election to select one receiver per mini-slot to resolve channel contention in the two-hop range of a node. We define the *priority* of receiver $x$ at mini-slot $t$ as:

$$prio_x = hash(x \oplus t) \tag{6}$$

where $x$ is the node ID, and $t$ is mini-slot number. Because each node has a unique hash code, Equation (6) guarantees that each receiver in the two-hop range will have a unique node priority in each mini-slot. Then we map the node priority to the mini-slot number of the RTR section, as Figure 5 shows.

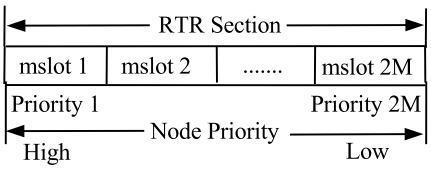


Fig. 5. Node priority and mini-slot mapping in RTR section

Given that the number of successful simultaneous transmissions in the two-hop range is at most twice the number of receive antennas ($M$), at most $2M$ receivers with the highest priorities should send the RTR packet. The length of the RTR section is $2M$ mini-slots. The RTR includes the channel scheduling, and the achieved spatial multiplexing gain ($G_{\mathrm{sm}}$) for the channel scheduling.

*4) Conflict scheduling result resolution:* Upon receiving RTRs from different receivers, nodes compare the $G_{\mathrm{sm}}$ of the RTR packets and follow the scheduling results corresponding to the larger $G_{\mathrm{sm}}$. When the $G_{\mathrm{sm}}$ of two RTRs are the same, then the links that are in conflict should not be used. Revisiting the example shown in Figure 4, after the relay scheduling, $r1$ sends an RTR with $G_{\mathrm{sm}}$, 4 while $r2$ sends an RTR with $G_{\mathrm{sm}}$ 3, then nodes $B, C, D$ will follow the scheduling result of $r1$.

*5) Packet scheduling:* Each node maintains packets in per-destination FIFO queues. The receiver indicates in the RTR which nodes can transmit and the sequence number (SN) of the packets which are intended to receive. A sender will discard the packets in the FIFO queue with smaller sequence number than the receiver has required.

### C. Scheduling based access

In the scheduling-based access period, the senders that find themselves in the scheduling result of the RTR without conflicts will transmit simultaneously using a single antenna. The length of scheduling based access period ($T_s$) is the remaining part of the time slot:

$$T_s = T - T_{\mathrm{rts}} - T_{\mathrm{rtr}} \tag{7}$$

The scheduling based access period is made up of multiple data slots. The length of a data slot ($T_{\mathrm{data}}$) is the time needed to send a data packet with maximum payload length. The number of the data slots ($D$) is:

$$D = \lfloor \frac{T_s}{T_{\mathrm{data}}} \rfloor \tag{8}$$

## V. NUMERICAL ANALYSIS

We compare the one-hop saturation throughput of CHAMP with a simple extension of IEEE 802.11 DCF (we denote it as DCF-MIMO) through numerical analysis. In DCF-MIMO, RTS/CTS handshake is used to eliminate the hidden terminal effect and the pilot symbols are sent in the RTS packet to the receiver. The RTS/CTS packets are sent with a low transmission rate ($R_{\mathrm{basic}}$), while the DATA/ACK packets are

sent with a high transmission rate ($R_{\text{data}}$) which utilizes the spatial multiplexing gain of MIMO links. DCF-MIMO is the most direct extension of IEEE 802.11 DCF for MIMO system.

### A. System Model and Assumptions

To compare the saturation throughput of CHAMP with DCF-MIMO in the single-hop scenario, we make the following assumptions, which are consistent with the previous numerical analysis of 802.11 DCF [12] [13]. We assume $N$ nodes located in the one-hop range of each other. All links are bidirectional or symmetrical. The channels are assumed to be error free and have no capture effects, so that collision of packets is the only source of errors.

### B. Saturated Throughput

We define the normalized system throughput ($S_{\text{norm}}$) as the total payload transmission time of the system over the time slot length:

$$S_{\text{norm}} = \frac{E[N_{\text{SDATA}}]E[\text{payload}]}{E[\text{length of a time slot}]} \tag{9}$$

where $E[N_{\text{SDATA}}]$ is the number of simultaneous transmissions, $E[\text{payload}]$ is the the payload information transmitted in a slot time. The actual system throughput ($S$) is defined as:

$$S = S_{\text{norm}} \times R \tag{10}$$

where $R$ is the physical layer transmission rate.

The saturation throughput analysis of DCF-MIMO is mainly based on the two-state Markov model developed in [12], which extends Bianchi's model [13] to take the impact of limited retransmit time of 802.11 DCF into account. In DCF-MIMO, $E[N_{\text{SDATA}}] = 1$.

For CHAMP, the probability that a node sends an RTS at a specific mini-slot during the RTS section ($P_{\text{RTS}}$) is:

$$P_{\text{RTS}} = \frac{1}{L} \tag{11}$$

The probability that an RTS transmission is successful ($P_{\text{SRTS}}$) is:

$$P_{\text{SRTS}} = C_N^1 P_{\text{RTS}}(1 - P_{\text{RTS}})^{(N-1)} \tag{12}$$

We denote the number of successful RTS transmissions by $N_{\text{SRTS}}$:

$$P_{\{N_{\text{SRTS}}=i\}} = C_L^i P_{\text{SRTS}}^i (1 - P_{\text{SRTS}})^{(L-i)} \tag{13}$$

where $i \in 0, \ldots, L$.

$$S_{\text{norm}} = \frac{E[N_{\text{SDATA}}]T_{\text{data}}}{T_{\text{RTS}} + T_{\text{RTR}} + T_{\text{data}}} \tag{14}$$

$$E[N_{\text{SDATA}}] = \sum_{j=0}^{M} j P_{\{N_{\text{SDATA}}=j\}} \tag{15}$$

For simplicity, we do not consider the effects of relay scheduling. Because the transmission of an RTR is collision-free by means of the receiver election in the two-hop range, and given that there are no hidden terminals in the one-hop range, which excludes the conflict scheduling result resolution, the probability of the number of scheduling transmissions ($P_{\{N_{\text{SDATA}}=j\}}$) is only dependent on the number of successful RTS transmissions ($P_{\{N_{\text{SRTS}}=i\}}$).

$$\begin{aligned} & E[N_{\text{SDATA}}] \\ &= \sum_{j=1}^{M}\sum_{i=1}^{L} jP_{\{N_{\text{SDATA}}=j|N_{\text{SRTS}}=i\}}P_{\{N_{\text{SRTS}}=i\}} \\ &= \sum_{j=1}^{M-1}\sum_{i=1}^{L} jP_{\{N_{\text{SDATA}}=j|N_{\text{SRTS}}=i\}}P_{\{N_{\text{SRTS}}=i\}} \\ &\quad + \sum_{i=1}^{L} MP_{\{N_{\text{SDATA}}=M|N_{\text{SRTS}}=i\}}P_{\{N_{\text{SRTS}}=i\}} \\ &= \sum_{i=1}^{M-1} iP_{\{N_{\text{SRTS}}=i\}} + M\sum_{i=M}^{L} P_{\{N_{\text{SRTS}}=i\}} \end{aligned} \tag{16}$$

The first part of Equation (16) represents the case that the number of successful RTS transmissions is smaller than the number of receive antennas, then $N_{\text{SDATA}} = N_{\text{SRTS}} = i$ ($i \in 1, \ldots, M-1$). The second part of Equation (16) represents the case that the number of successful RTS transmissions is more than the number of receive antennas, then $N_{\text{SDATA}} = M$, $N_{\text{SRTS}} = i$ ($i \in M, \ldots, L$). With the increase of the RTS section length ($L$), the probability that an RTS transmission is a success also increases, but the ratio of the payload transmission time during a time slot decreases. There is a trade-off between $L$ and normalized system throughput, as Figure 6(a) shows. In this paper, we set $L = 30$.

### C. Physical layer transmission rate comparison

The physical layer transmission rate is:

$$R = C \times BW \tag{17}$$

where $C$ is the channel capacity, $BW$ is the channel bandwidth. In order to make a fair comparison between the MIMO and the virtual MIMO system, we assume that both systems have the same total bandwidth and unit variance noise. There is no spatial interference and both systems can achieve their channel capacity upper bounds. Hence, from Equation (1) and (17), we can get an approximate relationship of total transmission rate of virtual MIMO ($R_{\text{vmimo}}$) and MIMO ($R_{\text{mimo}}$) system:

$$\frac{R_{\text{vmimo}}}{R_{\text{mimo}}} \approx \frac{log(1+P)}{log(1+P/N)} \tag{18}$$

Based on the default transmission power and data-rate settings in Qualnet simulator [14], which are indicated in

Table III, we can obtain the transmission rate comparison of MIMO and virtual MIMO systems with different number of antennas, as Figure 6(b) shows. It demonstrates that MIMO system always achieves a lower total transmission rate than virtual MIMO system. The ratio of $R_{\mathrm{vmimo}}$ over $R_{\mathrm{mimo}}$ increases with the number of antennas but decreases with the additional transmission power.

TABLE III
TX POWER AND TX DATA RATE RELATIONSHIP

| Tx power(dBm) | Tx data Rate (Mbps) |
|---|---|
| 20.0 | 6, 9 |
| 19.0 | 12, 18 |
| 18.0 | 24, 36 |
| 16.0 | 48, 54 |

Now we assume that $R_{\mathrm{mimo}}$ is fixed at 54 Mbps and vary the number of receive antennas. Then, according to Figure 6(b), we can get the corresponding transmission rate of the virtual MIMO system ($R_{\mathrm{vmimo}}$) and maximum transmission rate of each link ($R_{\mathrm{link}}$), as Table IV shows.

TABLE IV
TX RATE OF VIRTUAL MIMO SYSTEM

| Number of antennas(M) | $R_{\mathrm{vmimo}}$ (Mbps) | $R_{\mathrm{link}}$ (Mbps) |
|---|---|---|
| 2 | 69.63 | 34.82 |
| 4 | 95.04 | 23.76 |
| 6 | 117.75 | 19.63 |

Based on the physical layer transmission rates in Table IV, we compare the saturation system throughput of CHAMP with DCF-MIMO, as Figure 6(c) shows, CHAMP increases the saturation throughput of the system significantly.

## VI. PERFORMANCE EVALUATION

In this section, we compare the performance of CHAMP with DCF-MIMO under multi-hop scenarios through simulations.

### A. Simulation settings

We assume each receiver has four receive antennas and is using 802.11a as the physical layer. The MIMO transmission rate is 54 Mbps. The transmit power is 16dBm. The receive threshold for 54Mbps data rate is -63dBm, the related transmission range is around 40m. All these simulation parameters are default settings in Qualnet simulator [14]. According to Table IV, the transmission rate of the virtual MIMO system is 95.04Mbps, while the maximum transmission rate for each link is 23.76Mbps. The duration of the simulation is 100 seconds. The simulations are repeated with ten different seeds to average the results for each scenario. We set the path loss factor $\alpha = 4$.

### B. Chain Topology

We first evaluate the performance of CHAMP in simple chain topologies. As Figure 7 shows, 11 nodes form a chain of 10 hops. We also randomly place some nodes in the one-hop transmission range of the chain which can be used as relay nodes. We set up a CBR/TCP flow over the chain and the flow length varies from 1 to 10 hops. Static routing is used to ensure the path $(C_1 \rightarrow C_2 \cdots \rightarrow C_{11})$ is chosen, which allows us to compare the performance without the influence of routing protocols. The traffic source continuously sends out data at the maximum possible rate so as to saturate the channel. The packet length is 1024 bytes.

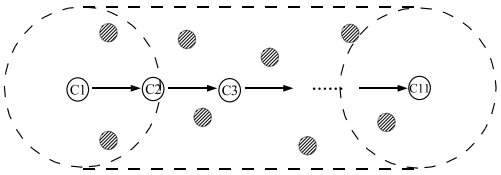


Fig. 7. Chain topology

Holland et al. [15] has shown that the throughput of CBR and TCP flows which are transmitted using 802.11 DCF will degrade rapidly when the number of hops along a chain increases. These are due to two reasons:

- The transmissions on a hop will inhibit other transmissions on other hops;
- Intermediate nodes of the chain can not send and receive at the same time;

The simulation results for CBR traffic are shown in Figure 8. The system throughput comparison of TCP traffic is shown in Figure 9(a). We can find through using virtual MIMO system, we not only increase the total physical layer transmission rate, but also the spatial reuse of the system. The cooperative transmission and multiple packet reception ability reduce the throughput degradation effect of the chain topology.

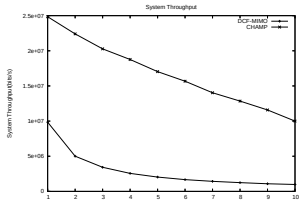


(a) Chain topology with TCP traffic

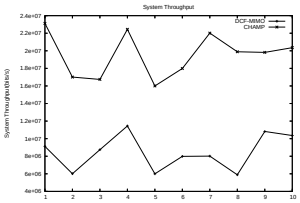


(b) Random topology with CBR traffic

### C. Random Topology

We generate 10 topologies with 50 nodes uniformly distributed across a 500 $\times$ 500 square meters area. We set up 20 CBR flows between randomly selected sender and receiver pairs which are more than two hops away from each other. The packet length of the CBR flow is 1024 bytes. The system throughput of each topology is shown in Figure 9(b), which demonstrates that CHAMP can increase the system throughput by at least two times, even in a random topology.

## VII. CONCLUSION

In this paper, we introduced CHAMP, a distributed channel scheduling protocol for ad hoc networks using virtual MIMO. CHAMP uses virtual antenna arrays to emulate the spatial

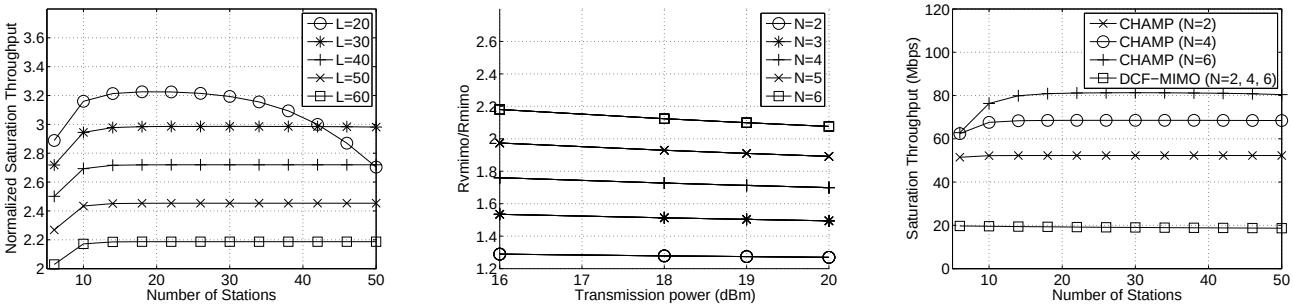


(a) Normalized System throughput vs. RTS section length ($L$)

(b) Tx rate comparison of MIMO and virtual MIMO

(c) Saturation throughput comparison

Fig. 6. Numerical analysis results

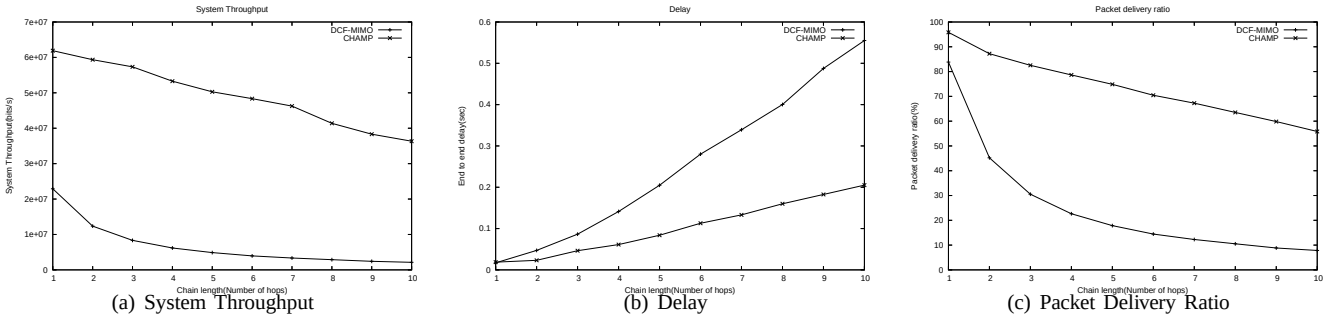


(a) System Throughput

(b) Delay

(c) Packet Delivery Ratio

Fig. 8. Chain topology with CBR traffic

multiplexing gain of MIMO links, which allows the receiver to decode the multiple transmissions simultaneously. Through cooperative transmission and distributed channel scheduling, CHAMP efficiently utilizes the multiple packet reception of the physical layer. Numerical analysis and simulation results demonstrate that it outperforms contention-based MAC protocol using MIMO links in single-hop and multi-hop scenarios.

## REFERENCES


[1] L. Zheng and D. Tse, "Diversity and Multiplexing: A Fundamental Tradeoff in Multiple-antenna Channels," *IEEE Transactions on Information Theory*, vol. 49(5), pp. 1073–1096, May 2003.

[2] G. Foschini, G. Golden, R. Valenzuela, and P. Wolniansky, "Simplified Processing for High Spectal Efficiency Wireless Communication Employing Multi-element Arrays," *IEEE J. Select. Areas Commun.*, vol. 17, pp. 1841–1852, Nov. 1999.

[3] J. Anderson, "Antenna Arrays in Mobile Communications: Gain, Diversity, and Channel Capacity," *IEEE Antennas and Propagation Magazine*, vol. 42, pp. 12–16, Apr 2000.

[4] K. Sundaresan, R. Sivakumar, M. A. Ingram, and T.-Y. Chang, "A Fair Medium Access Control Protocol for Ad-hoc Networks with MIMO links," in *Proceedings of IEEE INFOCOM*, March 2004, pp. 2559–2570.

[5] M. Hu and J. Zhang, "MIMO Ad Hoc Networks: Medium Access Control, Satuation Throughput, and Optimal Hop Distance," *Special Issue on Mobile Ad Hoc Networks, Journal of Communications and Networks*, 2004.

[6] J.C.Mundarath, P. Ramanathan, and B. Veen, "NULLHOC: a MAC protocol for adaptive antenna array based wireless Ad Hoc networks in multipath environments," in *Proceeding of IEEE Global Telecommunications Conference*, 2004, pp. 2765–2769 Vol.5.

[7] J.-S. Park, A. Nandan, M. Gerla, and H. Lee, "SPACE-MAC: Enabling Spatial Resuse using MIMO Channel-aware MAC," in *Proceeding of IEEE International Conference on Communications*, 2005.

[8] M. Dohler, *Virtual Antenna Arrays*. King's College London: Ph.D. Thesis, 2003.

[9] G.Jakllari, S.Krishnamurthy, M.Faloutsos, P.Krishnamurthy, and O.Ercetin, "A Framework for Distributed Spatio-Temporal Communications in Mobile Ad hoc Networks," in *Proceedings of IEEE INFOCOM*, 2006.

[10] G. J. Foschini and M. J. Gans, "On Limits of Wireless Communications in a Fading Environment when using Multiple Antennas," *Wireless Personal Communications*, no. 6, pp. 311–355, 1998.

[11] E. Telatar, "Capacity of Multi-antenna Gaussian Channels," *European Transactions on Telecommunications*, vol. 10, no. 6, pp. 585–595, November 1999.

[12] H. Wu and et al, "Performance of reliable transport protocol over IEEE 802.11 wireless LAN: Analysis and enhancement," in *Proc. INFOCOM*, New York, USA, June 2002.

[13] G. Bianchi, "Performance analysis of the IEEE 802.11 distributed coordination function," *IEEE Journal on Selected Areas in Communications*, vol. 18, no. 3, pp. 535–547, March 2000.

[14] Qualnet Simulator, "Scalable Network Technologies, http://www.scalable-networks.com/."

[15] G. Holland and N. Vaidya, "Analysis of TCP performance over mobile Ad Hoc networks," in *Proceedings of the 5th annual ACM/IEEE international conference on Mobile computing and networking(MobiCom)*, New York, USA, 1999, pp. 219–230.